Monthly Notices
of the
ROYAL ASTRONOMICAL SOCIETY

MNRAS **459,** 1415–1421 (2016)
Advance Access publication 2016 March 28

doi:10.1093/mnras/stw683

Remnant planetary systems around bright white dwarfs

Sara D. Barber,[1⋆†] Claudia Belardi,[1,2] Mukremin Kilic[1⋆] and A. Gianninas[1]

[1]*Homer L. Dodge Department of Physics and Astronomy, University of Oklahoma, 440 W. Brooks St., Norman, OK 73019, USA*
[2]*Department of Physics and Astronomy, University of Leicester, University Road, Leicester LE1 7RH, UK*

Accepted 2016 March 20. Received 2016 March 20; in original form 2015 June 19

ABSTRACT

We cross-correlate several sources of archival photometry for 1265 bright ($V \sim 16$ mag) white dwarfs (WDs) with available high signal-to-noise spectroscopy. We find 381 WDs with archival *Spitzer*+IRAC data and investigate this subsample for infrared excesses due to circumstellar dust. This large data set reveals 15 dusty WDs, including three new debris discs and the hottest WD known to host dust (WD 0010+280). We study the frequency of debris discs at WDs as function of mass. The frequency peaks at 12.5 per cent for 0.7–0.75 $M_\odot$ WDs (with 3 $M_\odot$ main-sequence star progenitors) and falls off for stars more massive than this, which mirrors predicted planet occurrence rates for stars of different masses.

Key words: white dwarfs – infrared: planetary systems – infrared: stars.

1 INTRODUCTION

Over the last two decades, hundreds of planets have been discovered and confirmed using a variety of techniques, each with its own set of advantages and shortcomings. The most intuitive method for detecting planets, of course, is to directly image them. Unfortunately, this method has also proven to be the most difficult. The small angular size of the orbit, in conjunction with the large contrast in brightness between the host star and planet place most systems beyond the resolution and photometric accuracy limit of current observational facilities (e.g. Graham et al. 2007). Observing a planetary transit, on the other hand, hinges on the slim chance of an alignment between the orbital plane and the observer's line of sight. For example, the probability of a Sun-like star being transited by a planet orbiting at 1 au is only 0.5 per cent. More distant planets, like Jupiter, are even less likely to transit. Similar to transits, radial velocity measurements require that the orbital plane be highly inclined. Furthermore, systems with low-mass planets and/or high-mass stars produce small velocity variation amplitudes, making them difficult to detect. Many of the hurdles facing main-sequence (MS) planet detections are compounded with increasing stellar mass. In fact, virtually no planets have been detected at stars more massive than 3 $M_\odot$.

Despite this bias in exoplanet detections, the frequency of Jovian planets increases from 3 per cent for M dwarfs to 14 per cent for 2 $M_\odot$ stars (Bowler et al. 2010; Johnson et al. 2010). Could it be that planets do not form around massive (>3 $M_\odot$) stars, or is this a selection effect? The planet formation models of Kennedy & Kenyon (2008) and Alibert, Mordasini & Benz (2011) suggest the latter. They predict that the fraction of stars with giant planets shows a steady increase with mass up to 3 $M_\odot$.

Since conventional planet detection techniques lose sensitivity in the massive (>3 $M_\odot$) regime, one can more easily search for planets by looking at these systems in post-MS. If planets survive post-MS evolution, they should be detectable around white dwarfs (WDs) (Burleigh, Clarke & Hodgkin 2002; Gould & Kilic 2008). Unfortunately, there are still no confirmed planetary mass objects around single WDs (Burleigh, Clarke & Hodgkin 2003; Friedrich et al. 2007; Faedi et al. 2011). The candidate planet around the pulsating WD GD 66 (Mullally et al. 2007) is currently disputed (Hermes 2013).

An easier way to detect remnant planetary systems around WDs is to look for the tidally disrupted remains of exoplanets, moons, and asteroids in the form of circumstellar debris discs (Debes & Sigurdsson 2002; Jura 2003; Kilic et al. 2006; Farihi, Jura & Zuckerman 2009; Veras et al. 2013, 2014a; Veras, Jacobson & Gänsicke 2014b). Consider a planetary system consisting of a WD, an asteroid-belt analogue and a Jupiter analogue. In this scenario, minor bodies are sent into chaotic orbits through repeated mean-motion resonance interactions with the Jupiter-like giant planet (Debes & Sigurdsson 2002; Jura 2003). In the event where the planetesimal crosses the tidal radius of its host WD, it is ripped apart. Subsequent passes further degrade the debris and it eventually embodies a disc geometry. Vanderburg et al. (2015) have recently identified the first disintegrating asteroid around the dusty WD 1145+017 (see also Gänsicke et al. 2016; Rappaport et al. 2016), providing support to this interpretation. The signature of a disc orbiting a WD is excess emission in the infrared due to the reprocessed light from this dust. This emission is spread out over a much larger area than the cross-sectional area of any planet, making it much brighter and easier to detect.

Interestingly, this method of detecting planet hosting systems probes a parameter space complementary to that available to

⋆ E-mail: sara.d.barber@ou.edu (SDB); kilic@ou.edu (MK)
† American Institute of Physics Congressional Fellow

ordinary planet searches. For instance, the signal strength of a circumstellar disc orbiting a WD does not decrease with increasing stellar mass. Also, contrary to transit and Doppler shift signals, the emission from a disc of tidally disrupted planetesimals is strongest when the orbital plane is face-on. Finally, planets that survive the red giant branch and asymptotic giant branch phases of stellar evolution likely lie several AU from the star (Burleigh et al. 2002). Thus, WD debris discs offer access to the otherwise elusive regime of planetary systems with massive host stars, face-on orbital planes, and large orbital separations.

Dust persists around a WD inside the tidal radius of the WD and outside the radius at which the equilibrium temperature is such that the dust will sublimate (2100 K for pure carbon dust; Debes et al. 2011). Some discs have been found to extend interior to this radius. Rafikov & Garmilla (2012) find that the dust sublimation temperature may be increased due to the vapour pressure of sublimated dust at the disc's inner rim. Poynting–Robertson drag carries dust from the tidal radius inward towards the WD, where viscous torques cause the sublimated dust to accrete on to the WD's surface (Rafikov 2011a,b; Metzger, Rafikov & Bochkarev 2012; Veras et al. 2013). This accretion results in a spectroscopically detectable pollution of the otherwise pristine WD atmosphere. Photospheric abundance analyses of polluted WDs show that the accreted metals originate from tidally disrupted minor bodies similar in composition to that of bulk Earth (Zuckerman et al. 2007; Dufour et al. 2010; Klein et al. 2011; Xu et al. 2014). Depleted levels of hydrogen and carbon rule out accretion of the interstellar medium (ISM) as a source of photospheric pollution (Jura 2006). Prior to this work, 39 WDs were known to host dust discs (Barber et al. 2014; Bergfors et al. 2014; Rocchetto et al. 2015). With this work, we explore the frequency of discs orbiting the greater DA WD population. We also probe, for the first time, a relatively large number of massive WDs for discs.

2 CROSS-CORRELATION

Gianninas, Bergeron & Ruiz (2011) conducted a spectroscopic survey of 1265 bright, hydrogen-atmosphere WDs from the 1999 incarnation of the McCook & Sion WD Catalog (McCook & Sion 1999). This survey contains 69 massive (>0.8 $M_{\odot}$) WDs and thus we are probing a large sample of massive WDs for the presence of dust for the first time.

We complement the broad-band *UBV* and Strömgren *uby* photometry from the McCook & Sion Catalog with a cross-correlation between several sources of archival data:

(i) Far- and near-UV photometry from the NASA Galaxy Evolution Explorer (*GALEX*; Bianchi, Conti & Shiao 2014) General Release 7

(ii) *ugriz* photometry from the Sloan Digital Sky Survey (SDSS; Ahn et al. 2014) Data Release 10

(iii) *JHK* photometry from the Two Micron All Sky Survey (2MASS; Skrutskie et al. 2006)

(iv) *YJHK* photometry from the UKIRT Infrared Deep Sky Survey (UKIDSS; Warren et al. 2007) Data Release 8

(v) 3.4 and 4.6 μm photometry from the *Wide-field Infrared Survey Explorer* (*WISE*; Wright et al. 2010) All-Sky Release

The results of our cross-correlation can be found in Table 1. We also have optical SDSS photometry for 708 of our targets, the crucial region of the spectral energy distribution to establish the expected near-infrared emission. We also have over a thousand detections in the ultraviolet with *GALEX* and the near-infrared with 2MASS and UKIDSS.

Table 1. Cross-correlation results.

Survey	Detections
GALEX	1055
SDSS	708
2MASS	970
UKIDSS	166

Table 2. IRAC detections.

Channel	Detections
1	304
2	377
3	156
4	228

Table 3. IRAC Ch 1 and Ch 2 photometry.

WD	$F_{3.6\,\mu m}$ (mJy)	$F_{4.5\,\mu m}$ (mJy)	$F_{5.8\,\mu m}$ (mJy)	$F_{8\,\mu m}$ (mJy)
0000+171	0.066(1)	0.044(1)	–	–
0001+433	0.019(2)	0.017(3)	0.030(14)	0.068(14)
0004+330	–	0.208(4)	–	0.053(13)
0009+501	–	0.969(3)	–	0.339(13)
0010+280	0.137(2)	0.088(2)	0.085(9)	0.067(12)
0011+000	0.235(6)	0.152(4)	–	–
0013−241	0.104(2)	0.066(1)	–	–
0018−339	0.189(2)	0.120(2)	–	–
0028−474	0.163(2)	0.105(1)	–	–
0032−175	0.336(2)	0.217(2)	0.126(6)	0.079(9)

Note. The remainder of this table is available online.

3 IRAC PHOTOMETRY

Mid-infrared photometry, like the 3.4 and 4.6 μm photometry available from *WISE*, is necessary to detect emission from a debris disc orbiting a WD. *WISE*, however, has poor spatial resolution (6 arcsec beam size) and is known to have a 75 per cent false positive rate for detecting dusty discs around WDs fainter than 14.5(15) mag in *W*1(*W*2) (Barber et al. 2014). To mitigate this high rate of spurious detections, we compile higher spatial resolution archival data from the InfraRed Array Camera (IRAC; Fazio et al. 2004a) on the *Spitzer Space Telescope*. We query the *Spitzer* Heritage Archive for any observations within 10 arcsec of the 1265 WDs from Gianninas et al. (2011) and find 907 Astronomical Observing Requests (AORs) for 381 WDs. Table 2 shows the number of detections we found in each IRAC band.

We use the IRAF `phot` and IDL `astrolib` packages to perform aperture photometry on the corrected basic calibrated data (CBCD) frames. We use a 2 pixel aperture and all Ch 1 photometry is corrected for the pixel-phase-dependence. The IRAC photometry for all 381 WDs can be found in Table 3.

A thorough analysis of all 1265 SEDs is beyond the scope of this work. Here, we focus only on those 381 WDs with *Spitzer* IRAC imaging as this data set is best suited for our goal, finding dusty debris discs. The parameter space spanned by our sample is presented in the histograms in Fig. 1, where the dark histogram represents the WDs we find to host dust. Our sample of WDs lies within 1800 pc and has a *V* magnitude distribution that peaks at 15.6 mag. The WDs range in temperature from 5.6 to 145 kK and in mass from 0.24 to 1.38 $M_{\odot}$.

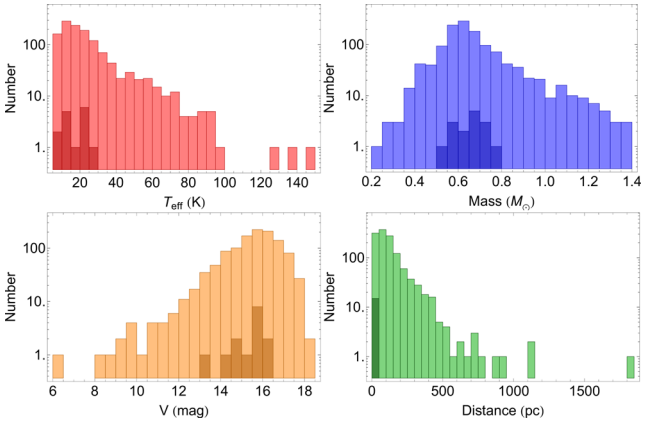

Figure 1. Histogram of effective temperature, mass, *V* magnitude, and distance for all 1265 WDs. The dark histogram indicates the parameter space occupied by the dusty WDs.

4 DISC MODELLING

We start by computing a synthetic spectrum for each WD based on the $T_{\rm eff}$ and log *g* values from Gianninas et al. (2011) and scale it to the SDSS *griz* photometry. If no SDSS data is available, we use the Strömgren *y*-band or broad-band *V*-band magnitude, where Strömgren photometry is prioritized over *V*-band photometry. In the case where more than one epoch of data is available, we plot all epochs rather than a weighted mean. Once the spectrum is scaled to the optical photometry, we measure any excess emission in the 2MASS, UKIDSS, *WISE*, and IRAC data. We then use a χ^2 minimization between the measured excess and a selection of dusty disc models. Our disc model grid includes inclinations of 0°–90° in steps of 10°, inner temperatures of 800–2100 K, outer temperatures of 100–1200 K in steps of 100 K and the constraint that the inner temperature exceed the outer temperature.

We use 2MASS and/or UKIDSS *JHK* photometry to constrain the inner radius of the disc. In all cases, the measured IRAC photometry is used to constrain the mid-IR portion of the SED. If PSF-fitting is required to remove a blend from the IRAC data, the photometry from the PSF-subtracted image is used. *WISE* data are not used in the fit but is still plotted for comparison.

5 RESULTS

5.1 Known discs

We find 15 WDs with circumstellar dust, 12 of which have been previously published. Fig. 2 shows an infrared colour–colour diagram for our WD targets based on UKIDSS and *WISE* photometry. Known dusty WDs in our sample (shown as red circles) have a relatively flat $J-H$ colour and positive $H-W2$ colour. Photometry for the remaining objects with positive $H-W2$ colours is likely contaminated by background objects in the large *WISE* beam. Using IRAC photometry, when available, we eliminate these sources as debris disc candidates. WD+M dwarf systems appear in a cluster at $H-W2=0.5$ mag and $J-H=0.5$ mag (Gianninas et al. 2011).

To display the robustness of our IRAC photometry and disc models, we check our IRAC photometry against the published photometry for the 12 previously known dusty WDs in Fig. 3(a). Our measurements agree with published values in all cases. We also compare our best-fitting disc parameters with published values in Fig. 3(b) and generally find agreement to within 5 per cent.

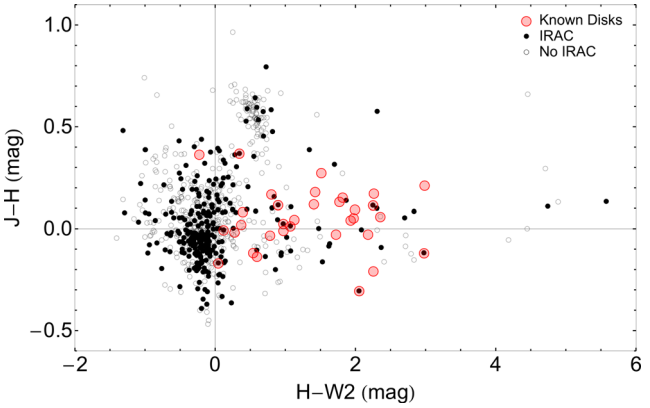

Figure 2. Infrared colours of our sample (black) compared with known dusty WDs (red). WDs with IRAC data are shown as filled points.

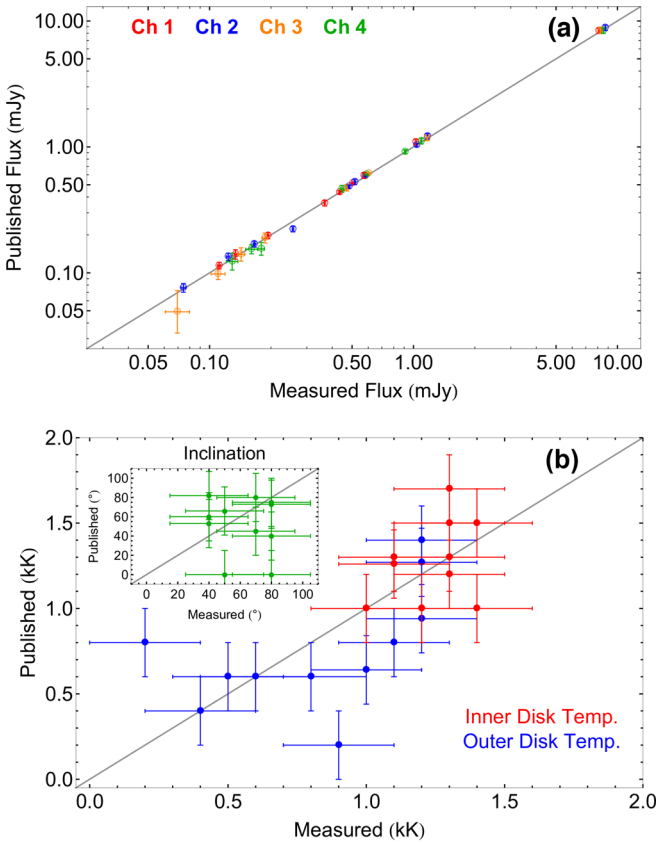

Figure 3. (a) Comparison between published IRAC photometry versus photometry we measure for the ten known dusty WDs in our sample with publicly available IRAC images in the *Spitzer* Heritage Archive. Our IRAC photometry agrees with published values. (b) Comparison of published disc parameters and our best-fitting disc parameters. Error bars show 200 K errors for disc temperatures and 25° errors for inclination. Grey lines indicate a one-to-one relation.

5.2 New discs

Our search also reveals three new dusty WDs, these spectral energy distributions can be found in Fig. 4. All three dusty WDs appear to host thin rings of circumstellar dust. The SED at WD 0010+280 matches that of a highly inclined disc, extending only 0.13 $R_\odot$ from the inner to outer radii. This WD has independently been found to host dust by Xu et al. (2015). Following

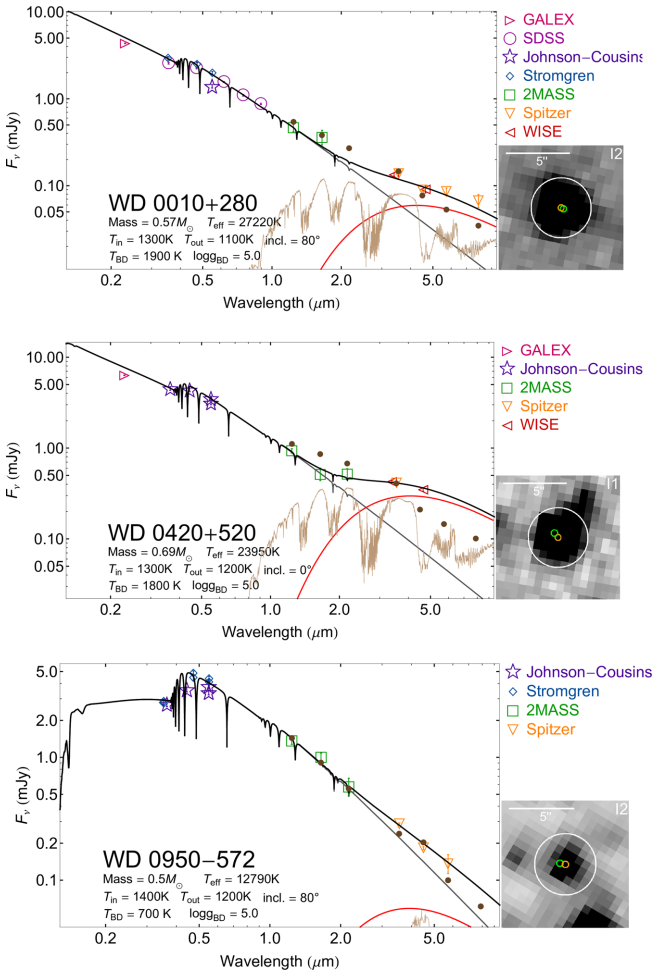

Figure 4. SED for three new dusty WDs. The photometry is shown as right triangles (*GALEX*), circles (SDSS), stars (Johnson–Cousins), diamonds (Stromgren), squares (2MASS), down triangle (*Spitzer*), and left triangle (*WISE*). The model WD atmosphere is shown by a grey line and the best-fitting debris disc model is shown by a red line. The addition of these two is shown by a the black line. The best-fitting brown dwarf model is shown by a brown line and the addition of the synthetic photometry of this model and the synthetic photometry of the model WD atmosphere is shown as brown points. In all cases, the measured excess more closely resembles the excess originating from a debris disc than that of a brown dwarf companion. The blending source in the J0420 IRAC 1 image is removed before PSF photometry is performed.

near-infrared UKIRT+WFCAM observations that reveal the disc, Xu et al. (2015) obtain high-resolution spectroscopy of this object using Keck+HIRES and find no trace of heavy element pollution. Thus, the origin of the measured excess remains unclear. However, we do not find any nearby sources contaminating the photometry. Furthermore, the *Spitzer* and *WISE* photometry are consistent. We measure the centroid position of the WD in the 2MASS *J*-band image and compare it with the position of the WD in the IRAC Ch 2 image and find that they are separated by 0.2 arcsec. Furthermore, according to the galaxy counts from Fazio et al. (2004b), there is only a 1.3 per cent chance of an alignment within our 2.4 arcsec aperture with a background galaxy bright enough to create the measured excess. Thus, we eliminate background galaxy contamination from consideration. WD 0010+280 is by far the hottest dusty WD found to date, a full 2000 K hotter than the 25 000 K WD 1537+515

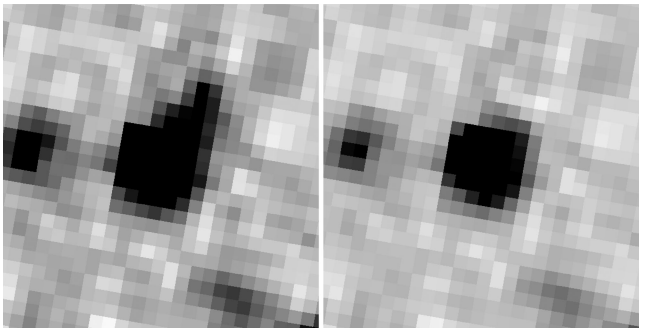

Figure 5. Original IRAC Ch 1 image (left) and PSF-subtracted image (right) for 0420+520. The blending source is successfully removed and the resultant photometry is virtually unchanged. The PSF-measured centroid of the 0.04 mJy blending source is separated from the WD's centroid by about 5 pixels.

Table 4. Best-fitting disc parameters.

WD	$T_{\rm in}$ (K)	$T_{\rm out}$ (K)	Incl. (°)	$R_{\rm in}$ ($R_\odot$)	$R_{\rm out}$ ($R_\odot$)
0010+280	1300	1100	80	0.52	0.65
0420+520	1300	1200	0	0.35	0.39
0950−572	1400	1200	80	0.17	0.21

Note. Typical uncertainties for disc inner and outer temperatures are 200 K and 20°–25° for inclination.

(Barber et al. 2014). Therefore, with this discovery we expand the parameter space occupied by dusty WDs.

We find that WD 0420+520 is surrounded by a thin, 0.05 $R_\odot$ wide, dusty disc. This object was first identified as a candidate WD+disc system using *WISE* by Hoard et al. (2013) and was recently found to have Ca absorption lines in its Keck+HIRES spectrum (Debes, private communication). There is a blended source in the IRAC Ch 1 photometry, but is cleanly subtracted (Fig. 5). We plot the photometry from the PSF-subtracted image in Fig. 4 and use it to fit the debris disc. Using the background galaxy counts from Fazio et al. (2004b), we estimate that the excess observed at WD 0420+520 has a 0.4 per cent chance of originating from a background galaxy. Further, we deem the 2MASS and IRAC centroids, separated by 0.47 arcsec, to be consistent (see Section 5.3).

The disc orbiting WD 0950-572 is the most narrow disc of the three, extending only 0.04 $R_\odot$. We examine the dependence of the WD centroid position on wavelength to see if a background galaxy might be the cause of the observed excess. After correcting the 2MASS *J*-band centroid for proper motion, we find that it differs from the IRAC Ch 2 centroid position by 0.44 arcsec. We also calculate that there is a 1.7 per cent chance of an alignment with a galaxy of the brightness needed to create the excess. Thus, we conclude that WD 0950-572 is a bona fide dusty WD. All of the new best-fitting disc parameters are listed in Table 4.

5.3 Centroid positions

We plot the 2MASS-IRAC centroid separations for all 15 dusty WDs in our sample in Fig. 6. The known dusty WDs appear as blue circles and the three new discs are red stars. We show the IRAC pointing accuracy as a green line and the mean separation for the known dusty WDs as a blue line, with a 1σ shaded area on either side. It is clear that the IRAC centroids for the three new disc hosting WDs are consistent with the 2MASS centroids within the

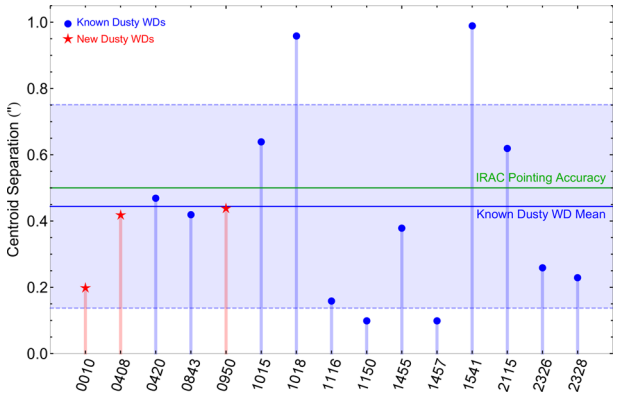

Figure 6. 2MASS versus IRAC centroid separations for each dusty WD corrected for proper motion. Centroids closer than 0.5 arcsec, the pointing accuracy of IRAC, are considered consistent. While the centroid separations of the dusty WDs, WD 1015 and WD 1541, are large they are within 2σ of the average separation of known dusty WDs.

errors. The risk of contamination due to the chance alignment with a background galaxy is of little concern with a sample of bright WDs.

Using the set of disc candidates with both *WISE* and IRAC photometry, we take advantage of the higher spatial resolution of IRAC to examine the contamination rate of *WISE*. We identify 34 disc candidates and find that 16 of these have neighbouring point sources within 6 arcsec, for a contamination rate of 50 per cent. These disc candidates, ranging 11.5–16.5 *W*1 mag, are brighter than the disc candidates from Barber et al. (2014) that revealed a 75 per cent *WISE* contamination rate. Our sample contains 374 WDs that are detected in archival IRAC 2 images. When we examine those brighter than $W2 = 15$ mag for blends, we find a contamination rate of 70 per cent.

5.4 Brown dwarfs

We consider brown dwarf companions as an alternate possible origin for the measured excesses around the three newly discovered dusty WDs. We compare each measured excess with the Burrows, Sudarsky & Hubeny (2006) solar metallicity, log g = 5.0, L and T dwarf spectral models. To find the best-fit brown dwarf model, we perform a chi-squared minimization between the 2MASS *JHK* and IRAC Ch 1 and Ch 2 synthetic photometry of the brown dwarf synthetic spectra and the corresponding WD measured photometric excesses. The synthetic spectrum is plotted in brown in Fig. 4. The brown points are the addition of the best-fitting brown dwarf synthetic photometry and the synthetic photometry of the WD model spectrum. The measured excesses more closely resemble the expected excess due to circumstellar dust than brown dwarf companions in all three cases. Therefore, the observed excesses are unlikely to be from brown dwarf companions.

5.5 Frequency dependence on mass

We report an overall disc frequency of 3.9 per cent, consistent with the 1–5 per cent disc frequency of previous surveys. Out of 381 WDs with IRAC data, 69 are massive (>0.8 $M_\odot$), thus this is the largest sample of massive WDs explored for the presence of dust. We find a signature for dust around none of these massive WDs, however. Assuming a 3 per cent frequency of discs for massive WDs (Barber et al., in preparation), there is a 12 per cent chance of finding zero discs in a sample of 69 WDs. Hence, the lack of detection of discs around massive WDs in our sample is not surprising. In fact, several WD infrared excess searches have returned a null result for dust orbiting massive WDs.

Hansen, Kulkarni & Wiktorowicz (2006) examined 12 hot ($T_{\rm eff} > 30\,000$ K), massive ($M > 1M_\odot$) WDs with *Spitzer* IRAC and found no instance of excess infrared emission. The authors were looking for planets, however, and we do not expect to find debris discs around stars this hot.

Mullally et al. (2007) surveyed 124 WDs with $T_{\rm eff} = 5000$–$170\,000$ K using mid-infrared *Spitzer* photometry. Their search for infrared excess finds two dusty WDs for a disc frequency of 1.6 per cent. However, this survey extends beyond the temperature range within which solid dust orbiting interior to the tidal radius can persist. While this sample was selected based on brightness, there are six WDs with $T_{\rm eff} = 9500$–$22\,500$ and $M > 0.8 M_\odot$ (Gianninas et al. 2011). None of these six WDs were found to have an infrared excess.

Farihi, Zuckerman & Becklin (2008) conducted a *Spitzer* IRAC survey that focused on descedents of intermediate-mass stars with $M > 3\,M_\odot$ and $T_{\rm eff} > 30\,000$ K. They found none of their 22 young, high-mass, field WDs to be dusty. This sample is also too hot for solid dust particles to persist within the stellar tidal radius.

Debes et al. (2011) recently searched for infrared excesses amongst an unbiased (in terms of metallicity) WD sample using the *WISE* (Wright et al. 2010) data. They found about 1–5 per cent of these WDs to be dusty. However, the large beam size of WISE allows for a 75 per cent false positive rate due to background contamination (Barber et al. 2014). Barber et al. (2014) conducted follow-up higher spatial resolution infrared imaging of 16 disc candidates from this study and confirm the observed infrared excess for one massive dusty WD, J1234.

We separate our IRAC sample into 0.05 solar mass bins and find that the frequency of discs peaks at 12.5 per cent for the 0.70–0.75 $M_\odot$ bin and drops off on either side (Fig. 7). We compute this frequency variation with progenitor mass using the initial–final mass functions of Kalirai et al. (2008) and Williams, Bolte & Koester (2009) and find general agreement between the two. To first order, the frequency–mass dependence resembles the dependence of giant planet formation on stellar mass put forth by Kennedy & Kenyon (2008), however larger sample sizes are required to narrow the confidence intervals. The number of WDs and disc detections in each bin and corresponding frequency with 1σ binomial confidence intervals (Burgasser et al. 2003; McCarthy & Zuckerman 2004) can be found in Table 5.

6 CONCLUSIONS

We create SEDs for 1265 bright WDs with precise atmospheric parameters using ultraviolet to mid-infrared photometry from *GALEX*, SDSS, 2MASS, UKIDSS, *WISE*, and *Spitzer*. We find 15 dusty WDs of which 12 are previously known and three are new detections. Our measured IRAC photometry of the 12 previously known dusty WDs as well as our best-fitting disc parameters agree with published values. All three new discs are narrow rings. We rule out contamination from chance alignment with background galaxies by comparing the centroid position of each WD in their 2MASS *J* and IRAC Ch 2 images. The presence of a galaxy, in all cases save an exact alignment with the WD, will shift the IRAC Ch 2 centroid (where an excess is measured) relative to the 2MASS *J* band centroid (where there is no excess). Centroids for all three new WDs are separated by less than 0.5 arcsec, the pointing accuracy of IRAC, and are thus considered consistent. We compare centroid separations for the new discs with

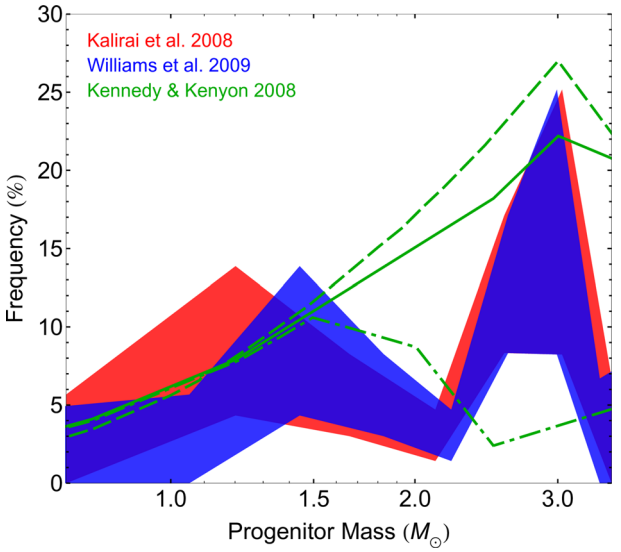

Figure 7. Frequency of discs as a function of WD progenitor mass according to the Kalirai et al. (2008) (red) and Williams et al. (2009) (blue) initial–final mass relations. The shaded region indicates the 1σ binomial confidence interval. The planet formation models of Kennedy & Kenyon (2008) are shown for reference in green where the solid and dashed lines assume an evolving snow line and the dash–dotted line assumes a static snow line. The WD disc frequency variation resembles that of MS giant planets, but larger sample sizes are required to narrow the confidence intervals.

Table 5. Frequency–mass variation.

Mass bin ($M_\odot$)	WDs	Discs	Freq. (per cent)	Confidence int. (per cent)
0.45–0.50	22	0	1.73	0.00–4.71
0.50–0.55	31	2	6.45	4.33–13.87
0.55–0.60	69	3	4.35	3.01–8.26
0.60–0.65	96	2	2.08	1.42–4.70
0.65–0.70	53	6	11.32	8.33–17.13
0.70–0.75	16	2	12.50	8.24–25.16
0.75–0.80	15	0	2.47	0.00–6.69
0.80–0.85	12	0	3.03	0.00–8.17

Note. Frequency–mass bins with a 68 per cent (1σ) binomial. confidence interval.

the 12 previously known discs and find that the mean separation of these centroids is also less than the IRAC pointing accuracy.

We find a disc frequency of 3.9 per cent for the subsample with *Spitzer* IRAC imaging, which is consistent with the 1–5 per cent frequency found in previous surveys (Mullally et al. 2007; Farihi et al. 2009; Debes et al. 2011; Barber et al. 2012; Rocchetto et al. 2015). We also find that the frequency varies with WD mass, though larger samples of WDs are required to precisely constrain the mass dependence. The frequency climbs slowly, peaks at 12 per cent in the 0.70–0.75 $M_\odot$ mass bin and falls off steeply for WDs more massive. This dependence closely mirrors the predicted frequency of giant planet formation as a function of MS mass put forth by Kennedy & Kenyon (2008). We find no dust around the massive WDs in our sample, but given the relatively small sample size, this is not surprising (Barber et al., in preparation).

ACKNOWLEDGEMENTS

We gratefully acknowledge the support of NASA and NSF under grants NNX14AF65G and AST-1312678, respectively.

This research has made use of the NASA/IPAC Infrared Science Archive, which is operated by the Jet Propulsion Laboratory, California Institute of Technology, under contract with the National Aeronautics and Space Administration.

This publication makes use of data products from the 2MASS, which is a joint project of the University of Massachusetts and the Infrared Processing and Analysis Center/California Institute of Technology, funded by the National Aeronautics and Space Administration and the National Science Foundation.

Based on observations made with the NASA Galaxy Evolution Explorer. *GALEX* is operated for NASA by the California Institute of Technology under NASA contract NAS5-98034.

This project uses UKIDSS data. The UKIDSS project is defined in Lawrence et al. (2007). UKIDSS uses the UKIRT Wide Field Camera (WFCAM; Casali et al. 2007). The photometric system is described in Hewett et al. (2006), and the calibration is described in Hodgkin et al. (2009). The pipeline processing and science archive are described in Hambly et al. (2008).

Funding for SDSS-III has been provided by the Alfred P. Sloan Foundation, the Participating Institutions, the National Science Foundation, and the U.S. Department of Energy Office of Science. The SDSS-III web site is http://www.sdss3.org/. SDSS-III is managed by the Astrophysical Research Consortium for the Participating Institutions of the SDSS-III Collaboration including the University of Arizona, the Brazilian Participation Group, Brookhaven National Laboratory, Carnegie Mellon University, University of Florida, the French Participation Group, the German Participation Group, Harvard University, the Instituto de Astrofisica de Canarias, the Michigan State/Notre Dame/JINA Participation Group, Johns Hopkins University, Lawrence Berkeley National Laboratory, Max Planck Institute for Astrophysics, Max Planck Institute for Extraterrestrial Physics, New Mexico State University, New York University, Ohio State University, Pennsylvania State University, University of Portsmouth, Princeton University, the Spanish Participation Group, University of Tokyo, University of Utah, Vanderbilt University, University of Virginia, University of Washington, and Yale University.

This publication makes use of data products from the *WISE*, which is a joint project of the University of California, Los Angeles, and the Jet Propulsion Laboratory/California Institute of Technology, and NEOWISE, which is a project of the Jet Propulsion Laboratory/California Institute of Technology. *WISE* and NEOWISE are funded by the National Aeronautics and Space Administration.

REFERENCES

Ahn C. P. et al., 2014, ApJS, 211, 17
Alibert Y., Mordasini C., Benz W., 2011, A&A, 526, A63
Barber S. D., Patterson A. J., Kilic M., Leggett S. K., Dufour P., Bloom J. S., Starr D. L., 2012, ApJ, 760, 26
Barber S. D., Kilic M., Brown W. R., Gianninas A., 2014, ApJ, 786, 77
Bergfors C., Farihi J., Dufour P., Rocchetto M., 2014, MNRAS, 444, 2147
Bianchi L., Conti A., Shiao B., 2014, AdSpR, 53, 900
Bowler B. P. et al., 2010, ApJ, 709, 396
Burgasser A. J., Kirkpatrick J. D., Reid I. N., Brown M. E., Miskey C. L., Gizis J. E., 2003, ApJ, 586, 512
Burleigh M. R., Clarke F. J., Hodgkin S. T., 2002, MNRAS, 331, L41
Burleigh M., Clarke F., Hodgkin S., 2003, Sci. Frontiers Res. Extrasolar Planets, 294, 111
Burrows A., Sudarsky D., Hubeny I., 2006, ApJ, 640, 1063
Casali M. et al., 2007, A&A, 467, 777
Debes J. H., Sigurdsson S., 2002, ApJ, 572, 556

Debes J. H., Hoard D. W., Wachter S., Leisawitz D. T., Cohen M., 2011, ApJS, 197, 38
Dufour P., Kilic M., Fontaine G., Bergeron P., Lachapelle F.-R., Kleinman S. J., Leggett S. K., 2010, ApJ, 719, 803
Faedi F., West R. G., Burleigh M. R., Goad M. R., Hebb L., 2011, MNRAS, 410, 899
Farihi J., Zuckerman B., Becklin E. E., 2008, ApJ, 674, 431
Farihi J., Jura M., Zuckerman B., 2009, ApJ, 694, 805
Fazio G. G. et al., 2004a, ApJS, 154, 10
Fazio G. G. et al., 2004b, ApJS, 154, 39
Friedrich S., Zinnecker H., Correia S., Brandner W., Burleigh M., McCaughrean M., 2007, in Napiwotzki R., Burleigh M. R., eds, 15th European Workshop on White Dwarfs Vol. 372, Astron. Soc. Pac., San Francisco, p. 343
Gänsicke B. T. et al., 2016, ApJ, 818, L7
Gianninas A., Bergeron P., Ruiz M. T., 2011, ApJ, 743, 138
Gould A., Kilic M., 2008, ApJ, 673, L75
Graham J. R. et al., 2007, BAAS, 39, 134.02
Hambly N. C. et al., 2008, MNRAS, 384, 637
Hansen B. M. S., Kulkarni S., Wiktorowicz S., 2006, AJ, 131, 1106
Hermes J. J., 2013, Am. Astron. Soc. Meeting Abstracts, 221, 424.04
Hewett P. C., Warren S. J., Leggett S. K., Hodgkin S. T., 2006, MNRAS, 367, 454
Hoard D. W., Debes J. H., Wachter S., Leisawitz D. T., Cohen M., 2013, ApJ, 770, 21
Hodgkin S. T., Irwin M. J., Hewett P. C., Warren S. J., 2009, MNRAS, 394, 675
Johnson J. A., Aller K. M., Howard A. W., Crepp J. R., 2010, PASP, 122, 905
Jura M., 2003, ApJ, 584, L91
Jura M., 2006, ApJ, 653, 613
Kalirai J. S. et al., 2008, ApJ, 676, 594
Kennedy G. M., Kenyon S. J., 2008, ApJ, 673, 502
Kilic M., von Hippel T., Leggett S. K., Winget D. E., 2006, ApJ, 646, 474
Klein B., Jura M., Koester D., Zuckerman B., 2011, ApJ, 741, 64
Lawrence A. et al., 2007, MNRAS, 379, 1599
McCarthy C., Zuckerman B., 2004, AJ, 127, 2871
McCook G. P., Sion E. M., 1999, ApJS, 121, 1
Metzger B. D., Rafikov R. R., Bochkarev K. V., 2012, MNRAS, 423, 505
Mullally F., Kilic M., Reach W. T., Kuchner M. J., von Hippel T., Burrows A., Winget D. E., 2007, ApJS, 171, 206
Rafikov R. R., 2011a, MNRAS, 416, L55
Rafikov R. R., 2011b, ApJ, 732, L3
Rafikov R. R., Garmilla J. A., 2012, ApJ, 760, 123
Rappaport S., Gary B. L., Kaye T., Vanderburg A., Croll B., Benni P., Foote J., 2016, MNRAS, 458, 3904
Rocchetto M., Farihi J., Gänsicke B. T., Bergfors C., 2015, MNRAS, 449, 574
Skrutskie M. F. et al., 2006, AJ, 131, 1163
Vanderburg A. et al., 2015, Nature, 526, 546
Veras D., Mustill A. J., Bonsor A., Wyatt M. C., 2013, MNRAS, 431, 1686
Veras D., Leinhardt Z. M., Bonsor A., Gänsicke B. T., 2014a, MNRAS, 445, 2244
Veras D., Jacobson S. A., Gänsicke B. T., 2014b, MNRAS, 445, 2794
Warren S. J. et al., 2007, preprint (arXiv:astro-ph/0703037)
Williams K. A., Bolte M., Koester D., 2009, ApJ, 693, 355
Wright E. L. et al., 2010, AJ, 140, 1868
Xu S., Jura M., Koester D., Klein B., Zuckerman B., 2014, ApJ, 783, 79
Xu S., Jura M., Pantoja B., Klein B., Zuckerman B., Su K. Y. L., Meng H. Y. A., 2015, ApJ, 806, L5
Zuckerman B., Koester D., Melis C., Hansen B. M., Jura M., 2007, ApJ, 671, 872

SUPPORTING INFORMATION

Additional Supporting Information may be found in the online version of this article:

Table 3. IRAC Ch 1 and Ch 2 photometry.
(http://www.mnras.oxfordjournals.org/lookup/suppl/doi:10.1093/mnras/stw683/-/DC1).

Please note: Oxford University Press is not responsible for the content or functionality of any supporting materials supplied by the authors. Any queries (other than missing material) should be directed to the corresponding author for the article.

This paper has been typeset from a TEX/LATEX file prepared by the author.